Inorganic Chemistry

ARTICLE

pubs.acs.org/IC

# Ditantalum Dinitrogen Complex: Reaction of $H_2$ Molecule with "End-on-Bridged" $[Ta^{IV}]_2(\mu\text{-}\eta^1\text{:}\eta^1\text{-}N_2)$ and Bis($\mu$-nitrido) $[Ta^{V}]_2(\mu\text{-}N)_2$ Complexes

Wenchao Zhang,[†] Yanhui Tang,[‡] Ming Lei,*[,†] Keiji Morokuma,[§,∥] and Djamaladdin G. Musaev*[,∥]

[†]State Key Laboratory of Chemical Resource Engineering, Institute of Materia Medica, College of Science, Beijing University of Chemical Technology, Beijing 100029, P.R. China

[‡]School of Materials Science & Engineering, Beijing Institute of Fashion Technology, Beijing 100029, P.R. China

[§]Fukui Institute for Fundamental Chemistry, Kyoto University, Kyoto 606-8103, Japan

[∥]Cherry L. Emerson Center for Scientific Computation, Emory University, Atlanta, Georgia 30322, United States

Supporting Information

**ABSTRACT:**

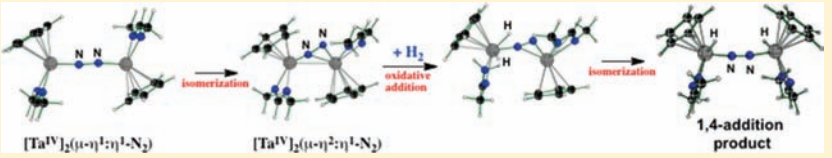


To elucidate (i) the physicochemical properties of the $\{(\eta^5\text{-}C_5Me_5)[Ta^{IV}](i\text{-}Pr)C(Me)N(i\text{-}Pr)\}_2(\mu\text{-}\eta^1\text{:}\eta^1\text{-}N_2)$, **I**, $[Ta^{IV}]_2(\mu\text{-}\eta^1\text{:}\eta^1\text{-}N_2)$, and $\{(\eta^5\text{-}C_5Me_5)[Ta^{V}](i\text{-}Pr)C(Me)N(i\text{-}Pr)\}_2(\mu\text{-}N)_2$, **II**, $[Ta^{V}]_2(\mu\text{-}N)_2$, complexes; (ii) the mechanism of the **I** → **II** isomerization; and (iii) the reaction mechanism of these complexes with an $H_2$ molecule, we launched density functional (B3LYP) studies of model systems **1**, **2**, and **3** where the $C_5Me_5$ and (*i*-Pr)C(Me)N(*i*-Pr) ligands of **I** (or **II**) were replaced by $C_5H_5$ and $HC(NCH_3)_2$, respectively. These calculations show that the lower-lying electronic states of **1**, $[Ta^{IV}]_2(\mu\text{-}\eta^1\text{:}\eta^1\text{-}N_2)$, are nearly degenerate open-shell singlet and triplet states with two unpaired electrons located on the Ta centers. This finding is in reasonable agreement with experiments [*J. Am Chem. Soc.* **2007**, *129*, 9284−9285] showing easy accessibility of paramagnetic and diamagnetic states of **I**. The ground electronic state of the bis($\mu$-nitrido) complex **2**, $[Ta^{V}]_2(\mu\text{-}N)_2$, is a closed-shell singlet state in agreement with the experimentally reported diamagnetic feature of **II**. The **1**-to-**2** rearrangement is a multistep and highly exothermic process. It occurs with a maximum of 28.7 kcal/mol free energy barrier required for the $(\mu\text{-}\eta^1\text{:}\eta^1\text{-}N_2) \rightarrow (\mu\text{-}\eta^2\text{:}\eta^2\text{-}N_2)$ transformation step. Reaction of **1** with $H_2$ leading to the 1,4-addition product **3** proceeds with a maximum of 24.2 kcal/mol free energy barrier associated by the $(\mu\text{-}\eta^1\text{:}\eta^1\text{-}N_2) \rightarrow (\mu\text{-}\eta^2\text{:}\eta^1\text{-}N_2)$ isomerization step. The overall reaction **1** + $H_2$ → **3** is exothermic by 20.0 kcal/mol. Thus, the addition of $H_2$ to **1** is kinetically and thermodynamically feasible and proceeds via the rate-determining $(\mu\text{-}\eta^1\text{:}\eta^1\text{-}N_2) \rightarrow (\mu\text{-}\eta^2\text{:}\eta^1\text{-}N_2)$ isomerization step. The bis($\mu$-nitrido) complex **2**, $[Ta^{V}]_2(\mu\text{-}N)_2$, does not react with $H_2$ because of the large energy barrier (49.5 kcal/mol) and high endothermicity of the reaction. This conclusion is also in excellent agreement with the experimental observation [*J. Am Chem. Soc.* **2007**, *129*, 9284−9285].

## 1. INTRODUCTION

Reduced nitrogen is an essential component of nucleic acids and proteins. A major fraction of all the nitrogen required for human nutrition is still obtained by biological nitrogen fixation.[1] The industrial analog of this process, in terms of N≡N triple bond utilization, is the old Haber−Bosch process.[2] Fixation of $N_2$ by $H_2$ in this heterogeneous catalytic process occurs via the formation of atomic nitrogen and hydrogen on the surface (via the on-surface atomization of the $N_2$ and $H_2$ molecules) followed by the addition of H-atoms to the coordinated nitrogen to form ammonia.[3] The atomization of $N_2$ on the surface was shown to be a slow step of the entire catalytic cycle. Empirically it has been found that the presence of potassium ions in the catalyst improves the efficiency of the process and is believed to promote the N≡N triple bond activation.[3]

While the heterogeneous Haber−Bosch catalyst is robust, it operates at high temperature and pressure, and is less energy- and atom-efficient. Therefore, it is of utmost necessity to find a soluble homogeneous version of the Haber−Bosch process that will (a) be more energy- and atom-efficient, (b) occur at milder experimental conditions, and (c) be amenable to detailed study and optimization. To this end, extensive studies[4−20] have led to the discovery of many fascinating new classes of homogeneous reactions involving the nitrogen molecule as a substrate.

One of such processes is the N≡N triple bond cleavage followed by utilization of the resulting metal-nitrido species in subsequent steps.[21] Another one is a coordination of dinitrogen molecule to

**Received:** May 30, 2011
**Published:** August 30, 2011

**Chart 1**

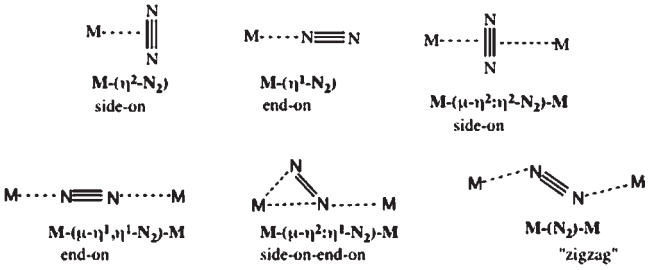


**Scheme 1**

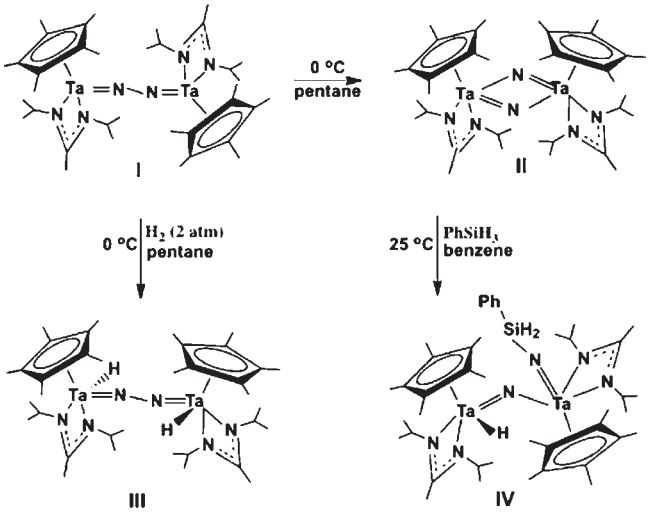


transition metal center and functionalization of the activated N≡N bond in various ways. Extensive experimental[6,7,9−17] and theoretical[8,18−20] studies have established that the $N_2$ molecule coordinates to transition metal center(s) via several modes (see Chart 1), and the N≡N bond activation and utilization mostly correlates with its coordination mode and the elongation of the N≡N bond.

In a majority of reported monotransition metal dinitrogen complexes, the $N_2$ molecule is coordinated to the metal center in end-on ($\eta^1$) manner, which can be utilized (for example, be converted to ammonia) mainly via the Chatt mechanism (i.e., via multiple protonation and reduction steps). However, in dinuclear transition metal complexes the $N_2$ molecule can coordinate to transition metal centers in multiple ways: side-on ($\mu$-$\eta^2$:$\eta^2$-manner), side-on-end-on ($\mu$-$\eta^2$:$\eta^1$-manner), end-on ($\mu$-$\eta^1$:$\eta^1$-manner), and zigzag. Furthermore, the side-on ($\mu$-$\eta^2$:$\eta^2$) or side-on-end-on ($\mu$-$\eta^2$:$\eta^1$) coordination of $N_2$ to transition metal centers leads to a more significant elongation and activation of its N≡N bond, mostly because of the strong back-donation from $d_\pi$-orbitals of the transition metal(s) to the $\pi^*$ orbital of N−N bond. A stronger M−$N_2$ interaction and significant N≡N bond activation in these complexes facilitates direct hydrogenation of the nitrogen molecule. There exist a few exceptions; for example, $N_2$ ligand in $[(\eta^5\text{-}C_9H_5\text{-}1\text{-}^I\text{Pr-}3\text{-Me})_2\text{Zr-NaX}]_2(N_2)$ (where X = Cl, Br and I) reported by Chirik and co-workers[17] is sandwiched between the Zr centers in the end-on fashion, but easily undergoes hydrogenation by an $H_2$ molecule. However, close examination shows that in this complex the $N_2$ ligand is also sandwiched between two Na centers in the side-on fashion. The existence of the Na-($\mu$-$\eta^2$:$\eta^2$)-Na bonding framework in this complex significantly contributes to activation of the end-on (relative to Zr centers) coordinated $N_2$ molecule. It is noteworthy that in this complex the Na ion most likely plays the same role as the potassium ion in the famous Haber−Bosch catalyst.

In spite of all the above-mentioned developments, the understanding of reactivity of transition metal-dinitrogen complexes still remains the focus of many research groups. In this aspect, a recent report by Sita and co-workers[13] on physicochemical properties and reactivity of the end-on-bridged $\{(\eta^5\text{-}C_5Me_5)[Ta^{IV}](i\text{-Pr})C(Me)N(i\text{-Pr})\}_2(\mu\text{-}\eta^1\text{:}\eta^1\text{-}N_2)$, **I**, complex, denoted below as $[Ta^{IV}]_2(\mu\text{-}\eta^1\text{:}\eta^1\text{-}N_2)$, is very intriguing (see Scheme 1). As reported by the authors, this species is stable and paramagnetic at <0 °C. However, the solid-state magnetic susceptibility (SQUID) data show that **I** may have a singlet ground state in the temperature range of 2−300 K. In other words, its singlet and triplet states could be very close in energy. Increasing the temperature from 0 °C (in pentane solution) results in conversion of **I** to diamagnetic species **II** (with a major *cis* conformer) with the following important geometrical parameters: $Ta^1$−$N^1$ ($Ta^2$−$N^2$) = 1.894(4) Å, $Ta^1$−$N^2$ ($Ta^2$−$N^1$) = 1.924(4) Å, $N^1$−$N^2$ = 2.574 Å. In **II**, the four-membered $[Ta]_2(\mu\text{-N})_2$ ring adopts a planar geometry. Furthermore, upon exposure to 2 atm $H_2$ gas compound **I** reacts slowly with an $H_2$ molecule at 0 °C, and provides a 43% yield of the single diastereomeric product **III**, along with a 20% yield of **II**. Interestingly, **II** does not react with $H_2$ under 2 atm at ambient temperatures and temperatures elevated to 60 °C, while *cis*-**II** reacts with $PhSiH_3$ to form **IV** with no bridging hydrides. Thus, these experimental findings raise several questions such as the following: (1) What is the electronic structure of the complexes **I** and **II**? (2) What are the mechanisms and relative energies of the reported **I** → **II** isomerization reaction? (3) What is the mechanism of the reaction **I** + $H_2$ → **III**?, and (4) Why complex **II** is less reactive toward $H_2$ molecule compared to complex **I**? Understanding these factors is vital and will allow us to better optimize reactivity of the $[Ta]_2(N_2)$ complexes, and provide reasonable guidance in design of $\eta^5$-cyclopentadienyl/$\eta^2$-aminate ligand based dinuclear dinitrogen complexes of groups 4, 5, and 6 metals.[22]

To answer the above-mentioned questions, we launched computational studies on the complexes **1**, **2**, **3**, and reactions **1** → **2**, **1** + $H_2$ → **3**, and **2** + $H_2$ → **3**. Here, structures **1**, **2**, and **3** are models of the experimentally reported complexes **I**, **II**, and **III**, respectively, where the $C_5Me_5$ and (*i*-Pr)C(Me)N(i-Pr) ligands of real systems are replaced by $C_5H_5$ and $HC(NCH_3)_2$ in model systems, respectively.

## II. COMPUTATIONAL PROCEDURES

All calculations were performed using the Gaussian 03 program.[23] The geometries of all species under investigation were optimized without any symmetry constraint at the B3LYP/{Lanl2dz (for Ta) + 6-31G* (for other atoms)} level of theory.[24,25] Below this method will be referred to as the "B3LYP/BSI" approach. For all species under investigation, Hessians were calculated and all transition states were confirmed to have one imaginary frequency corresponding to the reaction coordinate. Previously the B3LYP method was found to be reliable for systems like those studied in this paper.[26] Intrinsic reaction


dx.doi.org/10.1021/ic201159z |*Inorg. Chem.* 2011, 50, 9481–9490

Table 1. Calculated Relative Energies[a] of Intermediates, Transition States and Products of the 1 → 2 Isomerization, As Well As Spin Density Distributions (in e) on Important Atoms of These Structures

| | | rel. energies | | spin distributions | | | | |
|---|---|---|---|---|---|---|---|---|
| struct. | electr. state | $\Delta H$ | $\Delta G$ | $\langle S^2\rangle$ | $Ta^1$ | $Ta^2$ | $N^1$ | $N^2$ |
| **1_*trans*** | $^1A_{op}$ | −0.3 | 0.6 | 1.02 | 1.09 | −1.09 | −0.08 | 0.08 |
| | $^1A$ | 23.9 | 24.5 | | | | | |
| | $^3A$ | 0.00 | 0.00 | 2.01 | 1.01 | 1.01 | −0.05 | −0.05 |
| | $^5A$ | 40.2 | 37.7 | 6.03 | 1.65 | 1.61 | 0.41 | 0.01 |
| **1_*cis*** | $^1A_{op}$ | −0.3 | −0.2 | 1.02 | 1.09 | −1.09 | −0.08 | 0.08 |
| | $^1A$ | 23.4 | 24.9 | | | | | |
| | $^3A$ | −0.4 | 0.00 | 2.01 | 1.01 | 1.01 | −0.05 | −0.05 |
| **TS(1−1a)** | $^1A_{op}$ | 21.8 | 24.8 | 1.01 | 0.93 | −1.04 | 0.00 | 0.08 |
| | $^3A$ | 21.6 | 24.2 | 2.01 | 0.86 | 1.09 | 0.01 | −0.07 |
| **1a** | $^1A$ | 16.3 | 21.5 | | | | | |
| | $^3A$ | 20.2 | 21.8 | 2.01 | 0.91 | 1.09 | −0.04 | −0.07 |
| **TS(1a-1b)** | $^1A_{op}$ | 26.1 | 28.7 | 0.97 | 0.86 | −0.73 | −0.09 | −0.07 |
| | $^3A$ | 26.7 | 30.0 | 2.04 | 0.87 | 1.21 | −0.09 | −0.11 |
| **1b** | $^1A$ | 10.7 | 14.7 | | | | | |
| | $^3A$ | 15.6 | 17.1 | 2.06 | 1.06 | 1.06 | −0.13 | −0.13 |
| **TS(1b-2)** | $^1A_{op}$ | 16.8 | 19.5 | 0.77 | −0.76 | 0.75 | 0.16 | −0.15 |
| | $^3A$ | 23.0 | 26.1 | 2.03 | 0.88 | 0.79 | 0.34 | −0.13 |
| **2_*trans*** | $^1A$ | −53.4 | −50.7 | | | | | |
| | $^3A$ | −2.1 | 0.01 | 2.03 | 0.13 | 0.39 | 0.56 | 0.57 |
| **2_*cis*** | $^1A$ | −51.5 | −49.1 | | | | | |
| | $^3A$ | −0.8 | 1.8 | 2.02 | 0.29 | 0.25 | 0.70 | 0.33 |

[a] In kcal/mol, relative to the $^3A$ state of the reactant **1_*trans***.

coordinate (IRC) calculations were performed to confirm the nature of the calculated transition state and intermediates connected by this transition state. The Cartesian coordinates of all optimized structures at the B3LYP/BSI level are presented in the Supporting Information.

## III. RESULTS AND DISCUSSION

**A. Electronic and Geometrical Structures of the Complexes 1 and 2.** In general, Ta centers of the end-on-bridged form of the reactant, **1**, could have +2, +3, +4, and +5 oxidation states formally with $d^3$, $d^2$, $d^1$, and $d^0$ electronic configurations, respectively. Consequently, **1** could have a septet, quintet, triplet, and singlet electronic states.

As seen from Table 1, the ground electronic states of both *cis* and *trans* conformers of **1** are the open-shell singlet and triplet states with two unpaired electrons located on the Ta centers (one on each Ta atom). At the enthalpy level the open-shell singlet state is only 0.3 kcal/mol lower in energy for both *trans* and *cis* isomers. Inclusion of entropy effects only slightly changes the energy gap between the open-shell singlet and triplet states of these species. The closed-shell singlet states of **1_*trans*** and **1_*cis*** are 23.9 (24.5) and 23.4 (24.9) kcal/mol higher than their triplet states, respectively (Here and below we will present energies as $\Delta H$ ($\Delta G$)). The quintet and septet states of **1_*trans*** are very high in energy, 40.2 (37.7) and 67.8 (63.5) kcal/mol, respectively. The use of the nonhybrid BLYP/BS1 approach does not change the above-reported energy order of the open-shell singlet, triplet, and closed-shell singlet states: at the nonhybrid BLYP/BS1 level the open-shell singlet state is still the ground state, the triplet state lies only 0.2(−0.5) kcal/mol higher(lower), and the closed-shell singlet state lies 12.0 (12.0) kcal/mol higher. These computational finding are in reasonable agreement with experimental findings[13] showing easy accessibility of both paramagnetic and diamagnetic states of **I**.

The calculated $Ta^1-N^1$ ($Ta^2-N^2$) and $N^1-N^2$ bond distances in **1_*trans*** are 1.831 and 1.277 Å for the closed-shell singlet state, 1.821 and 1.285 Å for the open-shell singlet state, 1.820 and 1.287 Å for the triplet state, 1.961 and 1.220 Å for the quintet state, and 2.119 and 1.181 Å for the septet state, respectively (see Figure 1). The calculated values for the energetically lowest singlet and triplet states are in good agreement with 1.807(2) and 1.313(4) Å reported experimentally.[13]

Analyses of spin densities for lower-lying electronic states of **1_trans** show that in its open-shell singlet state $Ta^1$ and $Ta^2$-centers have one $\alpha$- and $\beta$-electrons, respectively, while at the triplet states each of them has one $\alpha$-spin (see Table 1). At the quintet and septet states N-atoms of $N_2$-unit acquire some (ca. 0.4 e) unpaired spins, and the amount of unpaired spins on $Ta^1$ and $Ta^2$-centers increases to 1.61 and 2.41e for the quintet and septet states, respectively. On the basis of the geometrical parameters [namely, the $Ta^1-N^1$ ($Ta^2-N^2$) and $N^1-N^2$ bond distances] and spin distributions, one can characterize the complex **1** as $Ta^{II/III}$---$(N_2)^-$---$Ta^{II/III}$ (at its septet state), $Ta^{III}$-$(N_2)^{2-}$-$Ta^{III}$ (at its quintet state), and $Ta^{IV}$═-$(N_2)^{4-}$═$Ta^{IV}$ (at its open-shell singlet and triplet states). Thus, **1** (at its both *trans* and *cis* isomers) is the $Ta^{IV}$═$(N_2)^{4-}$═$Ta^{IV}$ complex.

Calculation of the *trans* and *cis* isomers of the four-membered metallacycle form of the reactant, **2**, shows that they have closed-shell singlet ground states, which lie 53.4 (50.7) and 51.5 (49.1)


dx.doi.org/10.1021/ic201159z |*Inorg. Chem.* 2011, 50, 9481–9490

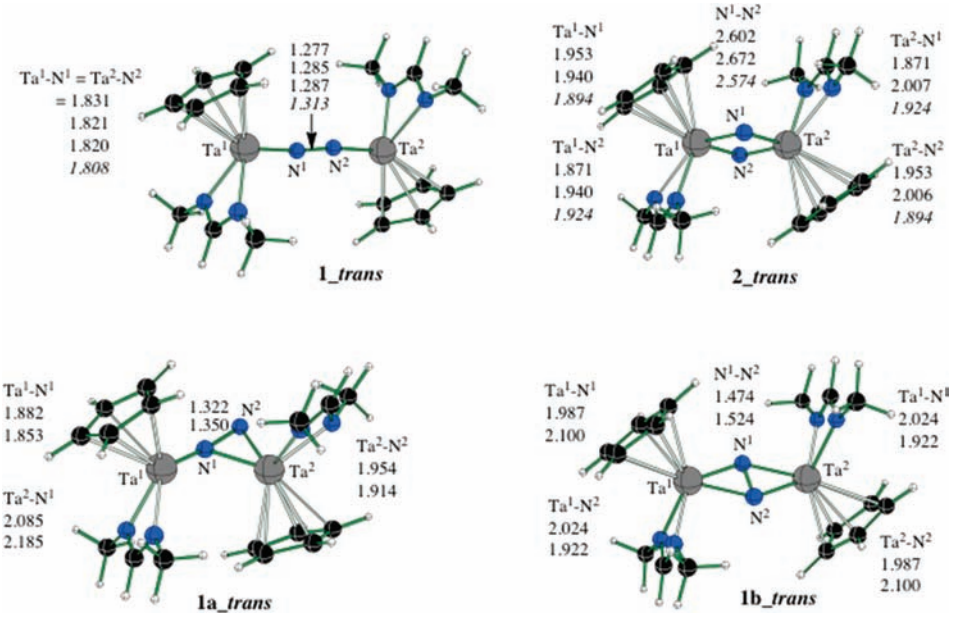


**Figure 1.** Calculated important geometry parameters of the *trans* isomers of complexes **1**, **1a**, **1b**, and **2**. Numbers in the first, second, and third rows are for the singlet, triplet, and quintet states, respectively, while the numbers in italic are the experimental values. Full geometrical parameters of these structures, as well as those for their *cis* isomers are given in the Supporting Information.

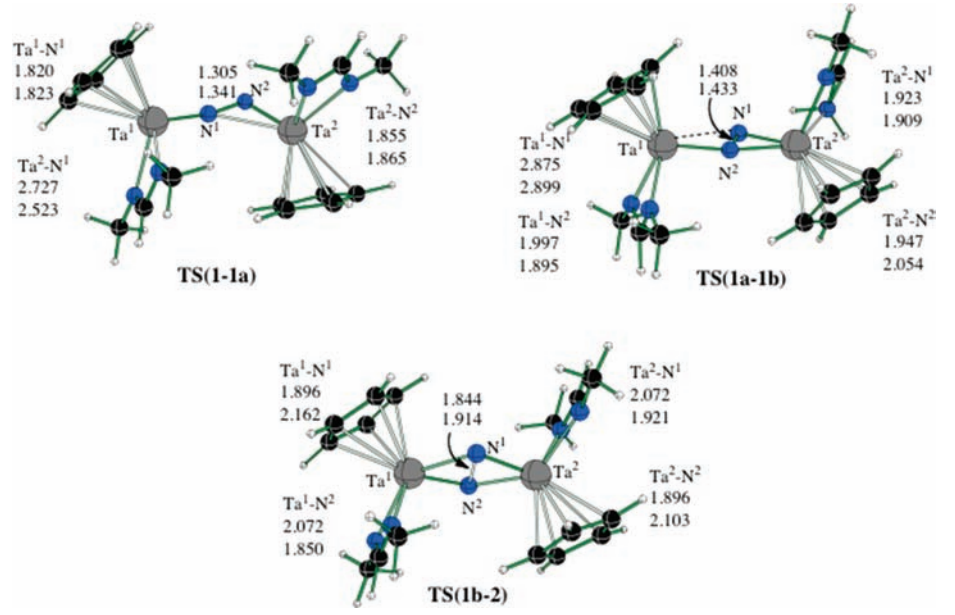


**Figure 2.** Calculated important geometry parameters of the *trans* isomers of transition states connecting complexes **1**, **1a**, **1b**, and **2**. Numbers in the first and second rows are for singlet and triplet states, respectively. Full geometry parameters of these structures, as well as those for their *cis* isomers are given in the Supporting Information.

kcal/mol lower in energy than the corresponding triplet states of **1**, respectively. The triplet states of **2_*trans*** and **2_*cis*** are 51.2 (50.7) and 50.8 (50.9) kcal/mol higher than their ground singlet states. As seen from Figure 1, the calculated $Ta^1-N^1/Ta^1-N^2$ bond distances are 1.953/1.871 Å and 1.940/1.940 Å, while the $Ta^2-N^1/Ta^2-N^2$ bond distances are 1.871/1.953 Å and 2.007/2.006 Å, in singlet and triplet states of **2_*trans***, respectively. These calculated geometrical parameters are in good agreement with the experimental[13] findings: $Ta^1-N^1/Ta^1-N^2$ = 1.894(4)/1.924(4) Å and $Ta^2-N^1/Ta^2-N^2$ = 1.924(4)/1.894(4) Å for compound **II**. Furthermore, the experimentally reported diamagnetic feature of **II** is consistent with the calculated singlet ground electronic state of **2**. On the basis of these geometry analyses, one may characterize the complex **2** as a $Ta^V$-$(N^{3-})_2$-$Ta^V$ complex.

**B. Mechanism of the 1 → 2 Isomerization Reaction.** As shown in Table 1, the **1** → **2** isomerization is highly exothermic, 53.4 (50.7) and 51.5 (49.1) kcal/mol, for *trans* and *cis* isomers, respectively, which is consistent with Sita et al.'s experimental finding[13] showing the conversion of **1** to **2** upon increasing the


dx.doi.org/10.1021/ic201159z |*Inorg. Chem.* 2011, 50, 9481–9490

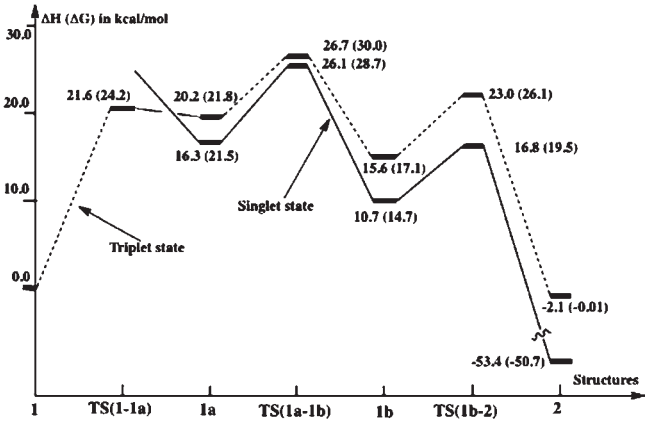


**Figure 3.** Schematic presentation of Potential Energy Surface (PES) of the **1** → **2** isomerization reaction.

temperature (in pentane solution). However, the mechanism of this transformation is not known, and the use of computation is necessary. For the sake of simplicity, below we discuss only the mechanism of the **1**_*trans* → **2**_*trans* isomerization, while that for the *cis* isomers is likely to be very similar. Therefore, below we will drop the "*trans*" extension in the notation, unless that is needed specifically.

Extensive computational studies revealed two intermediates on the potential energy surface of the **1** → **2** isomerization reaction (see Figure 1). Intermediate **1a** is a side-on-end-on ($\mu$-$\eta^2$:$\eta^1$) complex and has a closed-shell singlet ground state. Its triplet state is calculated to be 3.9 (0.3) kcal/mol higher than the ground singlet state. This intermediate lies 16.3 (21.5) kcal/mol higher than the ground triplet state of **1**. The calculated N−N bond distance in the singlet and triplet states of **1a**, 1.322 and 1.350 Å, is slightly longer than 1.277 and 1.287 Å for **1**, respectively. Thus, upon **1** → **1a** isomerization the N−N bond is partly activated.

The transition state connecting **1** and **1a** is structure **TS(1−1a)** with the N−N bond distance of 1.305 and 1.341 Å for singlet and triplet states, respectively (see Figure 2). Comparison of **TS(1−1a)** with reactant **1** reveals the bending of the $\angle N^1-N^2-Ta^2$ angle from about 173° to 123.4° and 102.6° for singlet and triplet states, respectively. The calculated barriers at these transition states (relative to reactant **1**) are 21.8 (24.8) and 21.6 (24.2) kcal/mol for open-shell singlet and triplet states, respectively. Thus, both **1** and **TS(1−1a)** have almost degenerate open-shell singlet and triplet states with two unpaired electrons, one on each Ta center. However, the ground state of the product **1a** is the closed-shell singlet state. This indicates a spin-flip after (or in the vicinity of) **TS(1−1a)** brings the product to the closed-shell singlet ground state. One should point out that the calculated imaginary frequencies (39.3*i* and 83.9*i* $cm^{-1}$ for singlet and triplet states, respectively) associated with the reaction coordinate at transition state **TS(1−1a)** are unexpectedly small, while they clearly correspond to the $Ta^2-N^1$ bond formation (coupled with a slight $N^1-N^2$ and $Ta^2-N^2$ bond elongation). The calculated small values of these normal-mode frequencies could be result of several factors including the following: (i) the reaction coordinate involves numerous heavy atoms (at least, 2 nitrogen and 2 tantalum), and (ii) the overall reaction **1** ($^3$**A**) → **1a** ($^3$**A**) is highly endothermic and the reverse barrier is only 1.4 (2.4) kcal/mol.

Another intermediate on the potential energy surface of the **1** → **2** isomerization is complex **1b**, which is connected to intermediate **1a** and final product **2** with transition states **TS(1a-1b)** and **TS(1b-2)**, respectively. The ground electronic state of **1b** is a closed-shell singlet state, and its triplet state lies 4.9 (2.4) kcal/mol higher. As seen in Figure 1, in **1b**, the $N_2$ unit is located between the two Ta centers and is coordinated to them in a side-on ($\mu$-$\eta^2$:$\eta^2$-) manner. In **1b**, the N−N bond distance is elongated to 1.474 and 1.524 Å from 1.305 and 1.341 Å in **1a**, for singlet and triplet states, respectively. In other words, in **1b** the N−N bond is a single bond. Thus, during the **1a** → **1b** transformation $N_2$ molecule moves from a side-on-end-on to side-on coordination mode. This process occurs via transition state **TS(1a-1b)**. Calculated geometrical parameters and normal-mode analyses confirm the nature of this transition state, which has only one imaginary frequency of 70.5*i* and 122.2*i* $cm^{-1}$ for singlet and triplet, respectively. Energy barriers at the singlet and triplet state of **TS(1a-1b)** are 26.1 (28.7) and 26.7 (30.0) kcal/mol, relative to the ground triplet state of **1**, and 9.8 (7.2) and 6.5 (8.2) kcal/mol, relative to the corresponding electron states of pre-reaction complex **1a**, respectively.

Intermediate **1b** converts to the product **2** via transition state **TS(1b-2)**, which can be characterized as the N−N single bond activation transition state. Indeed, as seen in Figure 2, at **TS(1b-2)**, N−N bond is significantly elongated (to 1.844 and 1.914 Å from 1.474 and 1.524 Å in **1b**, for singlet and triplet states). IRC calculations along the normal modes (489.2*i* and 440.9*i* $cm^{-1}$ for singlet and triplet, respectively) confirm that **TS(1b-2)** connects **1b** and **2**. Energy barriers at the singlet and triplet states of **TS(1b-2)** are 16.8 (19.5) and 23.0 (26.1) kcal/mol, relative to the ground triplet state of **1**, and 6.1 (4.8) and 7.4 (9.0) kcal/mol relative to the corresponding electron states of pre-reaction complex **1b**, respectively.

As shown in Figure 3, the overall **1** → **2** isomerization is highly exothermic, 53.4 (50.7) kcal/mol, and proceeds with maximum of 26.1 (28.7) kcal/mol energy barrier at the singlet transition state **TS(1a-1b)**, which corresponds to transformation of the N═N double bond to the N—N single bond and reorganization of the side-on-end-on complex to the side-on complex.

**C. Reactivity of the Complexes 1, 1a, 1b, and 2 toward $H_2$ Molecule.** *C.1. Mechanism of the Reactions of* ***1*** *and* ***1a*** *with $H_2$ Molecule.* The above presented results show that the $N_2$ molecule in the model complex $\{(\eta^5\text{-Cp})[Ta^{IV}][HC(NCH_3)_2\}_2(N_2)$ could be in three different coordination modes: ($\mu$-$\eta^1$:$\eta^1$-$N_2$), **1**, ($\mu$-$\eta^2$:$\eta^1$-$N_2$), **1a**, and ($\mu$-$\eta^2$:$\eta^2$-$N_2$), **1b**. Therefore, we study $H_2$ addition to each of these isomers and to the bis($\mu$-nitrido) complex **2**, $[Ta^V]_2(\mu\text{-N})_2$, which is another isomer of **1**. It is noteworthy to mention that experiments[13] have shown that upon exposure to 2 atm $H_2$ gas compound **1** reacts slowly with $H_2$ molecule and leads to the 1,4-addition product **3**. However, compound **2** does not react with $H_2$ under 2 atm at ambient temperature and temperature elevated to 60 °C.

Since open-shell singlet and triplet states of **1** are nearly degenerate, here we discuss the reactivity of triplet **1** (which is characterized as $Ta^{IV}$═$(N_2)^{4-}$═$Ta^{IV}$ complex) with $H_2$ molecule for simplicity. As seen in Figure 4, the first stage of this reaction is oxidative addition of the H−H bond to one of the Ta centers, that is, dihydrogen → dihydride transformation. In this figure, for the sake of simplicity of presentation, we omitted the Cp-rings and $HC(NCH_3)_2$ ligands wherever possible. Oxidative addition of $H_2$ to $Ta^1$ occurs with a 16.9 (27.0) kcal/mol


dx.doi.org/10.1021/ic201159z |*Inorg. Chem.* 2011, 50, 9481–9490

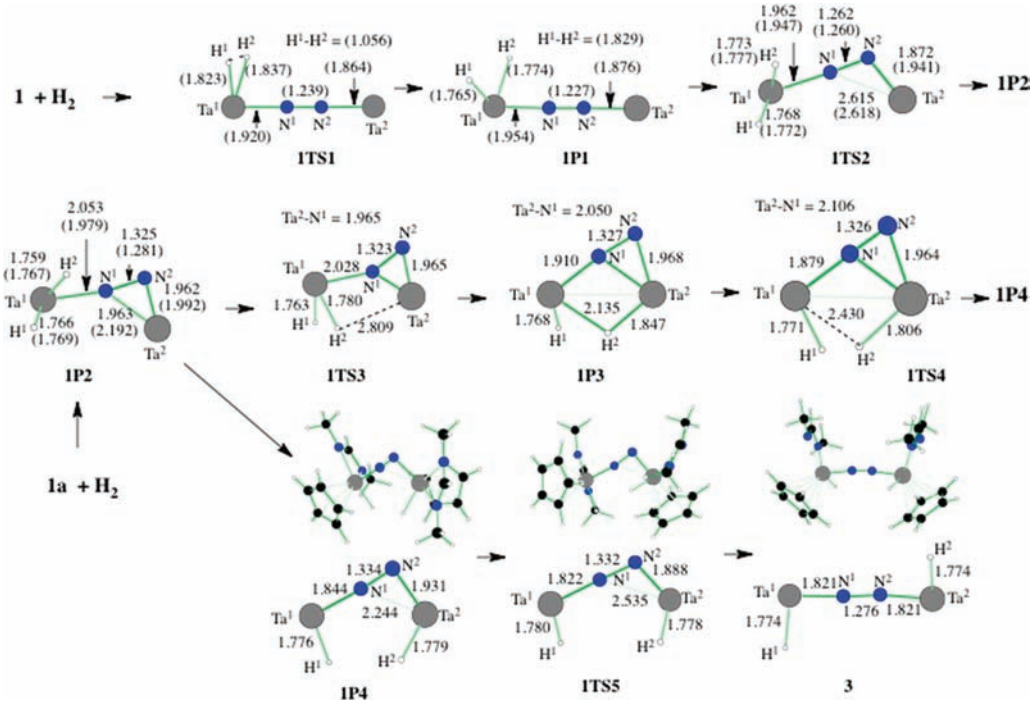


**Figure 4.** Calculated important geometry parameters of intermediates, transition states, and products of the reactions **1** + $H_2$ and **1a** + $H_2$. Numbers given without and with parenthesis are for singlet and triplet states, respectively. Full geometry parameters of these structures, as well as those for their *cis* isomers are given in the Supporting Information.

**Table 2. Calculated Relative Energies[a] of Intermediates, Transition States, and Products of the Reactions 1_*trans*/1a_*trans* + $H_2$ → 3, As Well As Spin Density Distributions (in e) on Important Atoms of These Structures**

| | | relative energies | | spin distributions | | | | | | |
|---|---|---|---|---|---|---|---|---|---|---|
| structure | electr. state | $\Delta H$ | $\Delta G$ | $\langle S^2 \rangle$ | $Ta^1$ | $Ta^2$ | $N^1$ | $N^2$ | $H^1$ | $H^2$ |
| **1**_*trans* + $H_2$ | $^3$A | 0.00 | 0.00 | 2.01 | 1.01 | 1.01 | −0.05 | −0.05 | | |
| **1TS1** | $^3$A | 16.9 | 27.0 | 2.02 | 0.04 | 1.41 | 0.41 | −0.08 | −0.00 | 0.09 |
| **1P1** | $^3$A | 12.2 | 21.9 | 2.02 | −0.10 | 1.44 | 0.48 | −0.05 | 0.00 | 0.07 |
| | $^1$A | 19.0 | 30.6 | 0.00 | | | | | | |
| **1TS2** | $^3$A | 32.9 | 44.4 | 2.02 | 0.00 | 1.26 | 0.46 | 0.06 | 0.01 | 0.06 |
| | $^1$A | 30.8 | 43.4 | 0.00 | | | | | | |
| **1P2** | $^3$A | 28.1 | 39.2 | 2.00 | 0.08 | 1.18 | 0.36 | 0.19 | 0.00 | 0.04 |
| | $^1$A | 12.4 | 25.5 | 0.00 | | | | | | |
| **1TS3** | $^1$A | 12.3 | 27.1 | 0.00 | | | | | | |
| **1P3** | $^1$A | −0.50 | 13.0 | 0.00 | | | | | | |
| **1TS4** | $^1$A | −0.60 | 13.4 | 0.00 | | | | | | |
| **1P4** | $^1$A | −2.60 | 9.50 | 0.00 | | | | | | |
| **1TS5** | $^1$A | −0.90 | 9.80 | 0.00 | | | | | | |
| **3** | $^1$A | −29.6 | −20.0 | 0.00 | | | | | | |

[a] In kcal/mol, relative to the $^3$A state of the reactants **1**_*trans* + $H_2$.

energy barrier at **1TS1** and is endothermic by 12.2 (21.9) kcal/mol. Here and below we use the **nAm** notation, where **n** stands for the reactant complex **1**, **1a**, **1b**, and **2**; **A** stands for the transition state (**TS**) and product (**P**), and **m** is the structure number. As seen in Figure 4, in **1TS1**, the calculated $H^1-H^2$, $Ta^1-H^1$, and $Ta^1-H^2$ bond distances are 1.056, 1.823, and 1.837 Å, respectively. In the dihydride product **1P1**, the $Ta^1-H^1$ and $Ta^1-H^2$ bond distances are 1.765 and 1.774 Å, respectively. It is interesting to note that the addition of H−H bond to $Ta^1$ destabilizes the $Ta^1-N^1$ bond and, consequently, stabilizes the $N^1-N^2$ bond: $N^1-N^2$ bond distance reduced from 1.287 Å in **1** to 1.227 Å in **1P1**. As seen in Table 2, in **1P1** the unpaired spins are distributed as follows: $Ta^1$ = 0.10 ($\beta$-spin), $Ta^2$ = 1.44 ($\alpha$-spin) and $N^1$ = 0.48 ($\alpha$-spin). Thus, on the basis of these geometry and spin distribution analyses, one can characterize the **1P1** mostly as a mixed-valent $(H)_2Ta^V$-$(N_2)^{3-}$=$Ta^{IV}$ complex with some (to a lesser extent) of $(H)_2Ta^{IV}\cdots(N_2)^-$-$Ta^{III}$ contribution.


dx.doi.org/10.1021/ic201159z |*Inorg. Chem.* 2011, 50, 9481–9490

The ground electronic state of **1P1** is the triplet state, while the singlet state lies only 6.8 (8.7) kcal/mol higher in energy (see Figure 5).

For the reaction to lead to the 1,4-addition product **3**, intermediate **1P1** has to transform to intermediate **1P2**, where $N_2$ is in the ($\mu$-$\eta^2$:$\eta^1$-$N_2$) coordination mode, as in compound **1a**. As expected, the singlet state of **1P2** is the ground state and lies 12.4 (25.5) kcal/mol higher than reactants $H_2$ + **1** ($^3$A). Its triplet state is 15.7 (13.7) kcal/mol higher in energy. The energy barrier associated with the reaction **1P1** → **1P2** is 11.8 (12.8) and 20.7 (22.5) kcal/mol at the singlet and triplet state transition states **1TS2**, respectively. Thus, the reaction starts from the triplet state reactants **1** + $\mathbf{H_2}$, proceeds on the triplet state surface and leads to the triplet state intermediate **1P1**. Then **1P1** converts to singlet state intermediate **1P2** via the singlet state transition state **1TS2**, which lies 30.8 (43.4) kcal/mol above the reactants **1** + $\mathbf{H_2}$. In other words, singlet and triplet state potential energy surfaces cross before the **1TS2**, and the system hops from triplet to singlet potential energy surface. Therefore, we discuss only the singlet state intermediates and transition states after the intermediate **1P2**. One should mention that the calculated important bond distances in **1P2** are consistent with its mostly $(H)_2Ta^V\cdots(N_2)^{4-}-Ta^V$ character which could also include (to a lesser extent) the mixed-valent $(H)_2Ta^V\cdots(N_2)^{3-}$--$Ta^{IV}$ character.

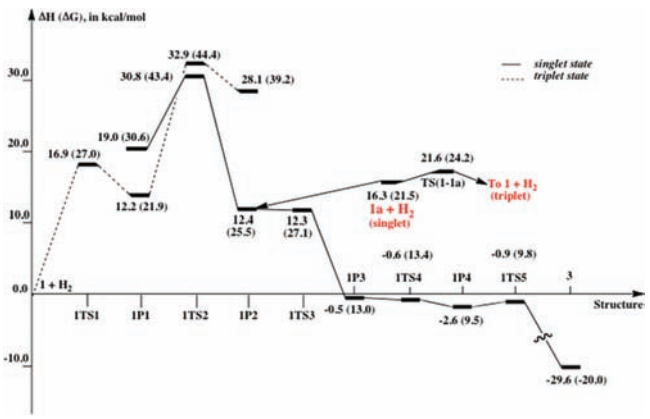


**Figure 5.** Schematic presentation of Potential Energy Surfaces (PES) of the reactions **1** + $H_2$ → **3** and **1a** + $H_2$ → **3**.

One should note that **1P2** could also be an intermediate for the direct addition of $H_2$ molecule to **1a**. This reaction occurs with a small (or no) energy barrier. Scanning potential energy surface of the reaction **1a** + $\mathbf{H_2}$ → **1P2** by fixing the H−H bond distance but optimizing all other geometrical parameters has produced no energy barrier (see Figure S1 of Supporting Information). Since the overall energy barrier, 30.8 (43.4) kcal/mol at the transition state **1TS2** required for the reaction **1** + $\mathbf{H_2}$ → **1P2**, is larger than 21.6 (24.2) kcal/mol at the **TS(1−1a)** required for the **1**-to-**1a** isomerization, the overall reaction **1** + $H_2$ → **1P2** is predicted to proceed via the pathway **1** + $H_2$ → **TS(1−1a)** + $H_2$ → **1a** + $H_2$ → **1P2**, which requires only 21.6 (24.2) kcal/mol energy at the transition state **TS-(1−1a)** and is endothermic by 12.4 (25.5) kcal/mol. *Thus, to add H−H bond to complex* ***1****, with an end-on* ($\mu$-$\eta^1$:$\eta^1$-$N_2$) *coordinated* $N_2$*-ligand, it first rearranges to the complex* ***1a*** *with an end-on-side-on* ($\mu$-$\eta^2$:$\eta^1$-$N_2$) *coordinated* $N_2$*-ligand, i.e., it undergoes the* ($\mu$-$\eta^1$:$\eta^1$-$N_2$) → ($\mu$-$\eta^2$:$\eta^1$-$N_2$) *isomerization.*

At the next stage, intermediate **1P2** rearranges to **1P3** via transition state **1TS3**. As seen in Figure 4, in **1P3** one of the H ligands ($H^2$) has moved from a terminal position on $Ta^1$ to bridging one between the Ta centers. As we have shown previously,[8a,b] this type of rearrangement occurs with a very small energy barrier and is slightly exothermic; for the present reaction the calculated barrier is only 0.1 (1.6) kcal/mol, and process **1P2** → **1P3** is exothermic by 12.9 (12.5) kcal/mol. The calculated energy difference between the **1**($^3$**A**) + $H_2$

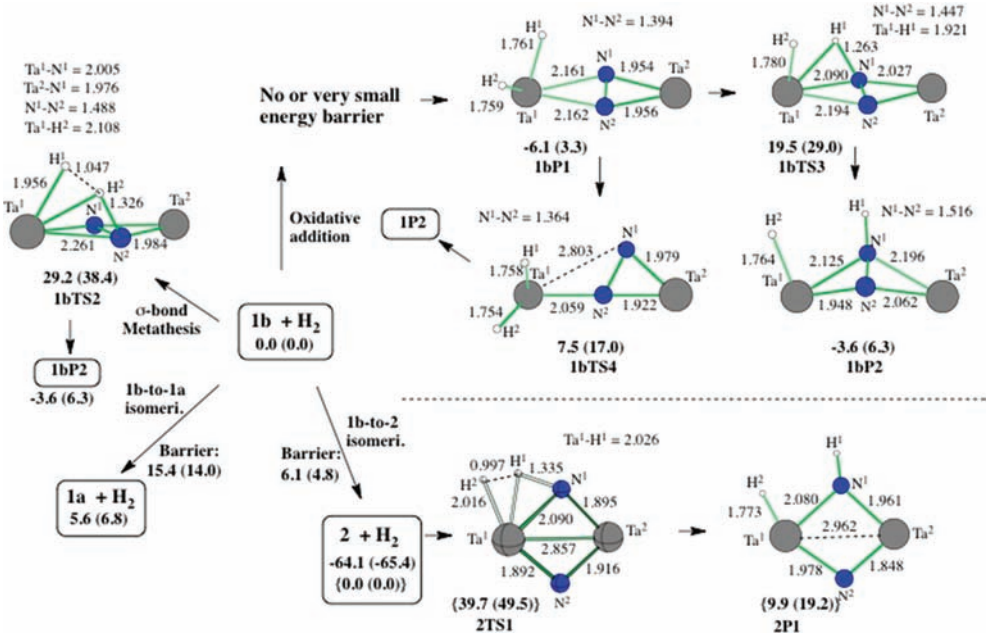


**Figure 6.** Calculated important geometry parameters (in Å) and relative energies (in kcal/mol) of intermediates, transition states, and products of the reactions **1b** + $\mathbf{H_2}$ and **2** + $\mathbf{H_2}$. Full geometry parameters and total energies of these structures, as well as those for their *cis* isomers are given in Supporting Information.


dx.doi.org/10.1021/ic201159z |*Inorg. Chem.* 2011, 50, 9481–9490

reactants and **1P3** intermediate is −0.5 (13.0) kcal/mol (see Figure 5).

The transfer of the bridging $H^2$ atom to the $Ta^2$ center in **IP3** to form intermediate **1P4** is extremely easy; it occurs with almost no barrier at enthalpy level (only 0.4 kcal/mol barrier at the $\Delta G$ level) at the transition state **1TS4** and is exothermic by 1.9 (9.5) kcal/mol. Intermediate **1P4**, which could be characterized mostly as $HTa^V$--$(N_2)^{4-}$--$Ta^VH$ complex, rearranges to another $HTa^V$--$(N_2)^{4-}$--$Ta^VH$ complex **3**, the final 1,4-addition product, with a 1.7 (0.3) kcal/mol energy barrier at the transition state **1TS5**. Reaction $\mathbf{1}(^3A) + H_2 \rightarrow \mathbf{3}$ is calculated to be highly exothermic, by as much as 29.6 (20.0) kcal/mol.

*In summary, reaction* $\mathbf{1}(^3A) + H_2 \rightarrow \mathbf{3}$*, that is, the 1,4-addition of* $H_2$ *to the complex* **1** *with an end-on* $(\mu\text{-}\eta^1\text{:}\eta^1\text{-}N_2)$ *coordinated* $N_2$*-ligand, proceeds with a maximum of 21.6 (24.2) kcal/mol energy barrier associated with the isomerization of reactant* **1** *to intermediate* **1a** *with a* $(\mu\text{-}\eta^2\text{:}\eta^1\text{-}N_2)$ *coordinated* $N_2$ *molecule, for example, the* $(\mu\text{-}\eta^1\text{:}\eta^1\text{-}N_2) \rightarrow (\mu\text{-}\eta^2\text{:}\eta^1\text{-}N_2)$ *isomerization. The overall reaction is exothermic by 29.6 (20.0) kcal/mol.* Thus, the calculations show that 1,4-addition of $H_2$ to **1** is kinetically and thermodynamically feasible. This conclusion is in good agreement with experiment.[13]

*C.2. Mechanisms of the Reactions of* **1b** *and* **2** *with* $H_2$ *Molecule.* In general, complex **1b**, the complex with the $(\mu\text{-}\eta^2\text{:}\eta^2\text{-}N_2)$ coordinated $N_2$-molecule, can react with $H_2$ molecule via several different pathways: (a) oxidative addition, which starts by oxidative addition of H−H bond to $Ta^1$ center, (b) $\sigma$-bond metathesis, where H−H bond simultaneously attacks to the $Ta^1$ and $N^1$ centers, (c) **1b**-to-**1a** isomerization followed by $H_2$ addition, and (d) **1b**-to-**2** isomerization followed by $H_2$ addition.

The oxidative addition of H−H bond to **1b** occurs with no (or very small) energy barrier; all attempts to locate the transition state corresponding to this step failed. Scanning of potential energy surface of the reaction $\mathbf{1b} + H_2 \rightarrow \mathbf{1bP1}$ by fixing the H−H bond distance but optimizing all other geometrical parameters produced no energy barrier (see Supporting Information, Figure S1). The intermediate of this oxidative addition reaction is **1bP1**, which lies 6.1 kcal/mol lower and 3.3 kcal/mol higher at the enthalpy and free energy levels, respectively. Rearrangement of **1bP1** to **1bP2** via transition state **1bTS3** or to **1P2** via transition state **1bTS4** requires 5.6 (32.3) and 13.6 (20.3) kcal/mol energy barrier, respectively, calculated relative to the ground singlet state of the intermediate **1bP1**. In other words, the oxidative addition of H−H bond to **1b** will only proceed via $\mathbf{1b} + \mathbf{H_2} \rightarrow \mathbf{1bP1} \rightarrow \mathbf{1bTS4} \rightarrow \mathbf{1P2}$ pathway with a 13.6 (20.3) kcal/mol energy barrier. In spite of the fact that this energy barrier is comparable to 15.4 (14.0) kcal/mol barrier required for the **1b**-to-**1a** isomerization, it is significantly larger than 6.1 (4.8) kcal/mol barrier required for **1b**-to-**2** isomerization (see Figure 3). In addition, while the **1b**-to-**1a** isomerization is 5.6 (6.8) kcal/mol endothermic, the **1b**-to-**2** isomerization is highly exothermic, by as much as 64.1 (65.4) kcal/mol. On the basis of these kinetic and thermodynamic considerations, it is most likely that **1b** will not react with $H_2$ molecule via the oxidative addition pathway before first converting to the bis($\mu$-nitrido) complex **2**.

The $\sigma$-bond metathesis pathway of the reaction $\mathbf{1b} + \mathbf{H_2}$, which requires 29.2 (38.4) kcal/mol energy barrier associated with the transition state **1bTS2** in its singlet ground state (see Figure 6) also cannot compete with the both **1b**-to-**1a** and **1b**-to-**2** isomerization reactions. Therefore, here we will not further discuss reaction $\mathbf{1b} + H_2$, although all calculated intermediates and transition states of this reaction are presented in Figure 6.

Bis($\mu$-nitrido) complex **2**, having two bridging N centers, reacts with $H_2$ molecule, like that reported for the group IV transition metal complexes,[8a−e,18,26] via $\sigma$-bond metathesis transition state **2TS1**, involving $Ta^1$ and $N^1$ centers of **2** and $H^1$ and $H^2$ atoms of the $H_2$ molecule. As seen in Figure 6, in **2TS1**, the calculated $H^1-H^2$, $N^1-H^1$, and $Ta^1-H^2$ bond distances are 0.997, 1.335, and 2.016 Å. IRC calculations along the normal mode vector ($1580i$ $cm^{-1}$) confirm that **2TS1** connects reactants $\mathbf{2} + H_2$ with product **2P1**. The calculated energy barrier at **2TS1** is 39.7 (49.5) kcal/mol, relative to the reactants $\mathbf{2} + H_2$. In the product **2P1**, one of the H atoms ($H^1$) is bound to $N^1$ atom, but the other one ($H^2$) is on the $Ta^1$ center. Reaction $\mathbf{2} + H_2 \rightarrow \mathbf{2P1}$ is found to be endothermic by 9.9 (19.2) kcal/mol. Thus, these results clearly show that the addition of $H_2$ to complex **2** is not feasible. This conclusion is in good agreement with experiments.[13]

## IV. CONCLUSIONS

From the above presented computational results and discussions, we may draw the following conclusions.

(1) The lower-lying electronic states of both *cis* and *trans* conformers of **1**, $[Ta^{IV}]_2(\mu\text{-}\eta^1\text{:}\eta^1\text{-}N_2)$, are nearly degenerate open-shell singlet and triplet states. Their closed-shell singlet states are $\Delta H$ = 23.9 ($\Delta G$ = 24.5) and 23.4 (24.9) kcal/mol higher in energy than the triplet states, respectively. These findings are in good agreement with experiments[13] showing easy accessibility of paramagnetic and diamagnetic states of **I**. However, the *trans* and *cis* isomers of bis($\mu$-nitrido) complex **2**, $[Ta^V]_2(\mu\text{-N})_2$, have closed-shell singlet ground states, with triplet states lying 51.3 (50.7) and 50.7 (50.9) kcal/mol higher in energy. The experimentally reported[13] diamagnetic feature of **II** is consistent with the calculated singlet ground electronic state of **2**.

(2) The *trans* and *cis* isomers of bis($\mu$-nitrido) complex **2**, $[Ta^V]_2(\mu\text{-N})_2$, lie 53.4 (50.7) and 51.5 (49.1) kcal/mol lower in energy than the corresponding complex $[Ta^{IV}]_2(\mu\text{-}\eta^1\text{:}\eta^1\text{-}N_2)$,**1**, respectively. The **1**-to-**2** rearrangement (or experimentally reported **I**-to-**II** rearrangement[13]) occurs with a maximum of 26.1 (28.7) kcal/mol energy barrier required for the $(\mu\text{-}\eta^1\text{:}\eta^1\text{-}N_2) \rightarrow (\mu\text{-}\eta^2\text{:}\eta^2\text{-}N_2)$ rearrangement at the transition state **TS(1a-1b)**. At the beginning, complex **1**, $[Ta^{IV}]_2(\mu\text{-}\eta^1\text{:}\eta^1\text{-}N_2)$, rearranges to intermediate **1a**, $[Ta^{IV}]_2(\mu\text{-}\eta^2\text{:}\eta^1\text{-}N_2)$, with a 21.6 (24.2) kcal/mol energy barrier at **TS(1−1a)**. Then, **1a** rearranges to intermediate **1b**, $[Ta^{IV}]_2(\mu\text{-}\eta^2\text{:}\eta^2\text{-}N_2)$, with a 9.8 (7.2) kcal/mol energy barrier. Complex **1b** is thermodynamically less favorable and converts to complex **2**, $[Ta^V]_2(\mu\text{-N})_2$, with a 6.1 (4.8) kcal/mol energy barrier.

(3) Reaction of $\mathbf{1}(^3A)$, $[Ta^{IV}]_2(\mu\text{-}\eta^1\text{:}\eta^1\text{-}N_2)$, with $H_2$ molecule to form the 1,4-addition product $[HTa^V]_2(\mu\text{-}\eta^1\text{:}\eta^1\text{-}N_2)$, **3**, proceeds with a maximum of 21.6 (24.2) kcal/mol energy barrier associated by the **1**-to-**1a**, that is, the $(\mu\text{-}\eta^1\text{:}\eta^1\text{-}N_2) \rightarrow (\mu\text{-}\eta^2\text{:}\eta^1\text{-}N_2)$, isomerization. Then, **1a**, a $[Ta^{IV}]_2(\mu\text{-}\eta^2\text{:}\eta^1\text{-}N_2)$ complex, oxidatively adds H−H bond to one of the Ta centers to form the dihydride derivative, the **1P2** complex, with mostly $(H)_2Ta^V\cdots(N_2)^{4-}-Ta^V$ character.


dx.doi.org/10.1021/ic201159z |*Inorg. Chem.* 2011, 50, 9481–9490

Later, the **1P2** converges to complex $HTa^{V}\cdots(N_2)^{4-}$--$Ta^{V}H$, **1P4** via the hydride migration from one of Ta centers to another. At the final stage, the **1P4** rearranges to another $HTa^{V}\cdots(N_2)^{4-}$--$Ta^{V}H$ complex **3**, the final 1,4-addition product. Overall reaction $\mathbf{1}(^3A) + H_2 \rightarrow \mathbf{3}$ is exothermic by 29.6 (20.0) kcal/mol. Thus, addition of $H_2$ to **1** is kinetically and thermodynamically feasible and proceeds via the $(\mu\text{-}\eta^1{:}\eta^1\text{-}N_2) \rightarrow (\mu\text{-}\eta^2{:}\eta^1\text{-}N_2)$ isomerization followed by $H_2$ addition. This conclusion is in excellent agreement with the experiment.[13]

(4) The thermodynamically most favorable isomer of $[Ta^{V}]_2(\mu\text{-}N)_2$ complex, that is, bis($\mu$-nitrido) complex **2**, with two bridging N atoms, cannot react with an $H_2$ molecule at moderate experimental conditions because of the existence of a large energy barrier, 39.7 (49.5) kcal/mol, associated with the $\sigma$-bond metathesis transition state **2TS1**, and the endothermicity of 9.9 (19.2) kcal/mol. This conclusion is also in excellent agreement with the experiment.[13]

The above presented data and discussion, once again, have demonstrated the complexity of structure−reactivity relation in transition-metal-dinitrogen systems. Comparison of the knowledge acquired from the current study on the $[Ta]_2(N_2)$ complex with that for group IV transition metal dinitrogen complexes,[8a−e,18,26] $[M(IV)][N_2]$ shows the utmost importance of the structural flexibility of the $[M-N_2]$ fragment and the easy availability of multiple oxidation states of the metal centers. The structural flexibility of the $[M-N_2]$ fragment not only facilitates realization of various possible coordination modes of $N_2$ molecule, eventually leading to either more reactive $[M, d^0]_2[(\mu\text{-}\eta^2{:}\eta^2\text{-}N_2)]$ complexes or dinitrogen-to-bis(nitrido)$[M, d^0]$ rearrangement, but also makes available the coordinatively and oxidatively unsaturated transition metal centers that are suitable for the facile oxidative addition of various $\sigma$-bonds. Of course, other factors (including, but not limited to, ligands manifesting in many different ways and countercation) may also be important for controlling the reactivity of the metal-dinitrogen complexes. These factors should be a subject of comprehensive experimental and theoretical investigations.

## ■ ASSOCIATED CONTENT

**Supporting Information.** (1) Completed ref. 23; (2) $\langle S^2\rangle$ values and total energies (Table S1) and Mulliken atomic spin densities (Table S2) for all reported structures; (3) Cartesian coordinates for all species reported in this paper (Table S3), and (4) Scanning of Potential Energy Surface of the reactions **1a + $H_2$** and **1b + $H_2$** along the $H^1\cdots H^2$ distance (Figure S1). This material is available free of charge via the Internet at http://pubs.acs.org.

## ■ AUTHOR INFORMATION

### Corresponding Authors

*E-mail: leim@mail.buct.edu.cn (M.L.), dmusaev@emory.edu (D.G.M.).

## ■ ACKNOWLEDGMENT

This work was in part supported by Beijing Nova Fund (2005B17), the National Natural Science Foundation of China (Grants 21072018 and 20703003), the Fundamental Research Funds for the Central Universities (Program No. ZZ1020), the National Basic Research 973 Program of China (Grant 2007CB714304). We also thank Chemical Grid Project at Beijing University of Chemical Technology (BUCT) for providing part of the computational resources. Acknowledgement is made by M.L. for Emerson Center Visiting Fellowship. We acknowledge NSF Grant CHE-0553581 and use of computational resources at the Cherry Emerson Center for Scientific Computation is also acknowledged.

## ■ REFERENCES

(1) (a) Eady, R. R. *Perspectives on Bioinorganic Chemistry*; JAI Press: Greenwich, CT, 1991, p 255; (b) Kim, J.; Rees, D. C. *Nature* **1992**, *360*, 553–560. (c) Kim, J.; Rees, D. C. *Science* **1992**, *257*, 1667–1682. (d) Chan, M. K.; Kim, J.; Rees, D. C. *Science* **1993**, *260*, 792.

(2) (a) Smil, V. *Enriching the Earth: Fritz Haber, Carl Bosch, and the Tranformation of World Food Production*; The MIT Press: Boston, MA, 2001. (b) Ertl, G. *Chem. Rec.* **2001**, *1*, 33–45. (c) Schlogl, R. *Angew. Chem., Int. Ed.* **2003**, *42*, 2004–2008.

(3) Ertl, G. *Angew. Chem., Int. Ed.* **2008**, *47*, 3524–3535.

(4) (a) Leigh, G. J. *Acc. Chem. Res.* **1992**, *25*, 177–181, and references therein. (b) Leigh, G. J. *Science* **1998**, *279*, 506–507.

(5) Eady, R. R. *Chem. Rev.* **1996**, *96*, 3013–3030.

(6) (a) Fryzuk, M. D.; Love, J. B.; Rettig, S. J.; Young, V. G. *Science* **1997**, *275*, 1445–1447. (b) Fryzuk, M. D. *Acc. Chem. Res.* **2009**, *42*, 127–133. (c) MacKay, B. A.; Fryzuk, M. D. *Chem. Rev.* **2004**, *104*, 385–401. (d) MacLachlan, E. A.; Fryzuk, M. D. *Organometallics* **2006**, *25*, 1530–1543. (e) Fryzuk, M. D.; Johnson, S. A. *Coord. Chem. Rev.* **2000**, *200−202*, 379–409. (f) MacKay, B. A.; Munha, R. F.; Fryzuk, M. D. *J. Am. Chem. Soc.* **2006**, *128*, 9472–9483.

(7) Nishibayashi, Y.; Iwai, S.; Hidai, M. *Science* **1998**, *279*, 540–542.

(8) (a) Basch, H.; Musaev, D. G.; Morokuma, K.; Fryzuk, M. D.; Love, J. B.; Seidel, W. W.; Albinati, A.; Koetzle, T. F.; Klooster, W. T.; Mason, S. A.; Eckert, J. *J. Am. Chem. Soc.* **1999**, *121*, 523–528. (b) Basch, H.; Musaev, D. G.; Morokuma, K. *J. Am. Chem. Soc.* **1999**, *121*, 5754–5761. (c) Basch, H.; Musaev, D. G.; Morokuma, K. *Organometallics* **2000**, *19*, 3393–3403. (d) Musaev, D. G.; Basch, H.; Morokuma, K. In *Computational Modeling of Homogeneous Catalysis*; Maseras, F., Lledos, A., Eds.; Kluwer Academic Publ.: Dordrecht, The Netherlands, 2002; pp 325−361. (e) Bobadova-Parvanova, P.; Wang, Q.; Morokuma, K.; Musaev, D. G. *Angew. Chem., Int. Ed.* **2005**, *44*, 7101–7103. (f) Yates, B. F.; Basch, H.; Musaev, D. G.; Morokuma, K. *J. Chem. Theory Comput.* **2006**, *2*, 1298–1316. (g) Martinez, S.; Morokuma, K.; Musaev, D. G. *Organometallics* **2007**, *26*, 5978–5986.

(9) Peters, J. C.; Cherry, J.-P. F.; Thomas, J. C.; Baraldo, L.; Mindiola, D. J.; Davis, W. M.; Cummins, C. C. *J. Am. Chem. Soc.* **1999**, *121*, 10053–10067.

(10) (a) Yandulov, D. M.; Schrock, R. R. *Science* **2003**, *301*, 76–78. (b) Yandulov, D. M.; Schrock, R. R. *Inorg. Chem.* **2005**, *44*, 1103–1117. (c) Yandulov, D. M.; Schrock, R. R.; Reingold, A. L.; Ceccarelli, C.; Davis, W. M. *Inorg. Chem.* **2003**, *42*, 796–813. (d) Ritleng, V.; Yandulov, D. M.; Weare, W. W.; Schrock, R. R.; Hock, A. S.; Davis, W. M. *J. Am. Chem. Soc.* **2004**, *126*, 6150–6163. (e) Schrock, R. R. *Acc. Chem. Res.* **2005**, *38*, 955–962.

(11) (a) Pool, J. A.; Lobkovsky, E.; Chirik, P. J. *Nature* **2004**, *427*, 527–530. (b) Knobloch, D. J.; Lobkovsky, E.; Chirik, P. J. *Nat. Chem.* **2010**, *2*, 30–35, and references therein. (c) Pool, J. A.; Bernskoetter, W. H.; Chirik, P. J. *J. Am. Chem. Soc.* **2004**, *126*, 14326–14327. (d) Hanna, T. E.; Lobkovsky, E.; Chirik, P. J. *J. Am. Chem. Soc.* **2004**, *126*, 14688–14689. (e) Bernskoetter, W. H.; Lobkovsky, E.; Chirik, P. J. *J. Am. Chem. Soc.* **2005**, *127*, 14051–14061. (f) Chirik, P. J.; Henling, L. M.; Bercaw, J. E. *Organometallics* **2001**, *20*, 534–544. (g) Pool, J. A.; Lobkovsky, E.; Chirik, P. J. *J. Am. Chem. Soc.* **2003**, *125*, 2241–2251. (h) Chirik, P. J. *Organometallics* **2010**, *29*, 1500–1517.

(12) Ding, K.; Pierpont, A. W.; Brennessel, W. W.; Lukat-Rodgers, G.; Rodgers, K. R.; Cundari, T. R.; Bill, E.; Holland, P. L. *J. Am. Chem. Soc.* **2009**, *131*, 9471–9472, and references therein.

(13) Hirotsu, M.; Fontaine, P. P.; Epshteyn, A.; Zavalij, P. Y.; Sita, L. R. *J. Am. Chem. Soc.* **2007**, *129*, 9284–9285.
(14) (a) Chatt, J.; Dilworth, J. R.; Richards, R. L. *Chem. Rev.* **1978**, *78*, 589–625.(b) Chatt, J. In *Nitrogen Fixation*; Stewart, W. D. P., Gallon, J. R., Eds.; Academic Press: New York, 1980; p 1.
(15) Holland, P. L. *Acc. Chem. Res.* **2008**, *41*, 905–914.
(16) Pun, D.; Lobkovsky, E.; Chirik, P. J. *J. Am. Chem. Soc.* **2008**, *130*, 6047–6054.
(17) Pun, D.; Bradley, C. A.; Lobkovsky, E.; Keresztes, I.; Chirik, P. J. *J. Am. Chem. Soc.* **2008**, *130*, 14046–14047.
(18) Musaev, D. G. *J. Phys. Chem. B* **2004**, *108*, 10012–10018.
(19) Miyachi, H.; Shigeta, Y.; Hirao, K. *J. Phys. Chem. A* **2005**, *109*, 8800–8808.
(20) Studt, F.; MacKay, B. A.; Fryzuk, M. D.; Tuczek, F. *Dalton Trans.* **2006**, 1137–1140.
(21) Fontaine, P. P.; Yonke, B. L.; Zavalij, P. Y.; Sita, L. R. *J. Am. Chem. Soc.* **2010**, *132*, 12273–12285.
(22) (a) Laplaza, C. E.; Cummins, C. C. *Science* **1995**, *268*, 861. (b) Laplaza, C. E.; Johnson, M. J. A.; Peters, J. C.; Odom, A. L.; Kim, E.; Cummins, C. C.; George, G. N.; Pickering, I. J. *J. Am. Chem. Soc.* **1996**, *118*, 8623. (c) Laplaza, C. E.; Odom, A. L.; Davis, W. M.; Cummins, C. C. *J. Am. Chem. Soc.* **1995**, *117*, 4999–5000. (d) Cui, Q.; Musaev, D. G.; Svensson, M.; Sieber, S.; Morokuma, K. *J. Am. Chem. Soc.* **1995**, *117*, 12366. (e) Johnson, A. R.; Davis, W. M.; Cummins, C. C.; Serron, S.; Nolan, S. P.; Musaev, D. G.; Morokuma, K. *J. Am. Chem. Soc.* **1998**, *120*, 2071. (f) Nishibayashi, Y.; Iwai, S.; Hidai, M. *Science* **1998**, *279*, 540–542.
(23) Frisch, M. J. et al. *Gaussian 03*, Revision C1; Gaussian, Inc.: Wallingford, CT, 2004.
(24) (a) Becke, A. D. *Phys. Rev. A* **1988**, *38*, 3098–3107. (b) Lee, C.; Yang, W.; Parr, R. G. *Phys. Rev. B* **1988**, *37*, 785–789. (c) Becke, A. D. *J. Chem. Phys.* **1993**, *98*, 1372–1380.
(25) (a) Hay, P. J.; Wadt, W. R. *J. Chem. Phys.* **1985**, *82*, 270–283. (b) Hay, P. J.; Wadt, W. R. *J. Chem. Phys.* **1985**, *82*, 299–310. (c) Wadt, W. R.; Hay, P. J. *J. Chem. Phys.* **1985**, *82*, 284–298.
(26) (a) Musaev, D. G.; Hirao, K. *J. Phys. Chem. A* **2003**in press. (b) Bach, R. D.; Gluhkovtsev, M. N.; Canepa, C. *J. Am. Chem. Soc.* **1998**, *120*, 775. (c) Lynch, B. J.; Fast, P. L.; Harris, M.; Truhlar, D. G. *J. Phys. Chem. A* **2000**, *104*, 4811. (d) Also see refs 8 and 18.
(27) Toomey, H. E.; Pun, D.; Veiros, L. F.; Chirik, P. J. *Organometallics* **2008**, *27*, 872–879.